Energy Conversion and Management 292 (2023) 117363

Contents lists available at ScienceDirect

Energy Conversion and Management

journal homepage: www.elsevier.com/locate/enconman

Techno-economic analysis of a novel retrofit solution for the domestic hot water system: A comparative study

Aminhossein Jahanbin [a,b,*], Giovanni Semprini [a], Maurizio Goni [a]

[a] Department of Industrial Engineering (DIN), Alma Mater Studiorum - University of Bologna, Viale Risorgimento 2, 40136 Bologna, Italy

[b] CIRI - Centro Interdipartimentale di Ricerca Industriale Edilizia e Costruzioni, Alma Mater Studiorum - University of Bologna, Via del Lazzaretto 15/5, 40131 Bologna, Italy

ARTICLE INFO

Keywords:
Domestic hot water
Energy efficiency
Retrofit solution
Storage tank
Economic analysis
Dynamic simulation

ABSTRACT

The retrofit solution for domestic hot water (DHW) system in existing buildings requires to ensure the long-term energy security and efficiency as well as to minimise occupants' disturbance, construction works and installation costs. In this regard, the present study performs a techno-economic evaluation on a novel retrofit solution for DHW production in a pilot building. The proposed solution appoints a substantial role to the thermal energy storage through a 2-pipe hot water network utilisable for both DHW and heating purposes. The first storage level is provided by a centralised buffer storage supplied by a PV-BESS-driven heat pump while the second level consists of decentralised modular tanks installed in each dwelling for the production and storage of hot water. Firstly, experimental thermal performance of the proposed decentralised storages is investigated. By developing a dynamic simulation code, the energy efficiency of the proposed solution is compared to that of the existing system in the pilot building as well to that of a typical centralised system as a benchmark solution. Finally, economic analysis of the retrofit solution is performed to address capital expenditures of the system, including purchasing and installation costs, as well as its life cycle cost (*LCC*). The obtained results indicate that the proposed system reduces the annual energy consumption for DHW production more than 7,200 kWh, with respect to the existing DHW system. Furthermore, it is shown that, in the proposed system, the fraction of thermal loss from piping network decreases by 31.5%, compared to a typical DHW centralised system. Economic assessment of the proposed solution implies that this system, in terms of both mechanical and electrical components, requires 13.7% lower initial investment than a typical centralised system. However, the cost of control systems in this system is higher since it is inherently a control-based system.

1. Introduction

The building sector is considered as one of the largest energy consuming sectors in European Union (EU) countries using approximately 40% of the total energy demand [1]. The European Commission has set several long and short-term goals to increase energy efficiency in buildings as well as to reduce the energy consumed by the building sector. The building's energy consumption is assessed by regarding the required energy for heating, cooling, ventilation, lighting, and domestic hot water (DHW). Space heating and DHW represent more than 80% of total domestic energy consumption and the major share of their demand is covered by heaters operated either by gas/oil or electricity [2]. The current energy proportion for DHW production in dwellings is likely to be augmented since the thermal resistance and air tightness of envelopes improve. Consequently, the share of energy devoted to the space heating and cooling tends to go down, making DHW as a dominant energy load in high-performance buildings, namely as high as 50% of total heat demand [3]. It is therefore of great importance to enhance energetic performance of DHW system and to optimise the DHW consumption while preserving constraints imposed by the rules [4].

Recent research in reduction of energy use in building has been primarily focused on the required load for space heating/cooling and ventilation, whereas current knowledge on the energy use and its optimisation for DHW production seems to be inadequate [5]. A review on available studies in the literature implies that the energy efficiency of existing DHW systems is surprisingly low and that a significant amount

* Corresponding author at: Department of Industrial Engineering (DIN), Alma Mater Studiorum - University of Bologna, Viale Risorgimento 2, 40136 Bologna, Italy.

E-mail address: aminhossein.jahanbin@unibo.it (A. Jahanbin).

https://doi.org/10.1016/j.enconman.2023.117363
Received 6 May 2023; Received in revised form 12 June 2023; Accepted 30 June 2023
Available online 4 July 2023

of heat is lost from the hot water before it reaches the draw-off points [6]. Furthermore, the efficiency of DHW production may vary to significant extent from case to case due to the large scattering of key parameters in the system such as the time-dependency of DHW consumption profile, distribution system and level of insulation [7]. It can be stated that production of DHW in residential buildings may become the next bottleneck towards the sustainable development appointed by the European Commission. Hence, novel technologies and optimisation of the entire chain of the hot water production system, in conjunction with the heating system, are required to meet the ambitious goals of the future building regulations.

To reduce the energy footprint of DHW systems in the residential sector, optimising strategies aim at recovering heat from wastewater at multiple levels [8–11], reducing thermal losses via efficient hot water distribution systems within buildings [11–14], decreasing hot water consumption via technological and behavioural measures [15,16], and producing hot water through sustainable and efficient technologies. The latter encompasses a wide range of technological aspects including various heat pump systems [17–20], District Heating (DH) [21,22], thermal-solar collectors and photovoltaic (PV) cells [23,24], phase change materials (PCMs) [25], and novel designs for the hot water storage [26–28].

For instance, Liu et al. [19] proposed an inverter-driven heat pump with a multi-tubular tube-in-tube heat exchanger for domestic hot water supply. The obtained results showed that their developed heat pump for DHW can provide hot water at 65 °C with larger heating COPs (coefficient of performance) compared to the COPs obtained by three existing heat pump systems, including a *trans*-critical CO_2, R410A with an indirect contact coil and a HFC125 heat pump. In another study, Huang et Al. [22] presented a novel charging method aiming at reducing the DH return temperature without violating the comfort or hygiene requirements. The proposed model employs the concept of multi-mode charging method considering the periodical characteristics of the load pattern. Various scenarios were simulated by a dynamic simulation model using the practical DHW load profiles from a case study. It was shown that the proposed charging method can reduce the primary return temperature by 5–8 °C compared to the conventional control method and that the distribution heat loss imposes a significant impact on the DH return temperature. Khoury et al. [27] developed an optimisation methodology for the Thermal Energy Storage (TES) tank embedded with PCMs for domestic water heating applications, with respect to the design parameter constraints and tank size. using adaptive simulated annealing algorithm, they found that the amount of available energy increases from 5 kWh to 7 kWh when using the multiple entry independent PCM modules, which was higher than the required energy.

Nevertheless, it is not yet clear which strategy or what combinations has more potential and may yield the best results for the least effort [29]. In the realm of DHW production and decarbonisation through efficient technologies, several studies focused on the integration of multiple technologies, whereas there is little to no research on the integrated effects of the proposed technology on whole-system comportment, particularly in-building interactions. This issue becomes more prominent when the discussion revolves around the retrofit solution for DHW system in existing buildings, where the adopted solution requires to ensure long-term energy security and efficiency as well as to minimise occupants' disturbance, construction works and installation costs. Furthermore, in terms of the retrofit solution for DHW system, the available studies in the literature mostly encompass an overall solution for heating, cooling and DHW production, which blurs the role of the proposed solution for specific-DHW issue. In this regard, the present study aims to examine the performance of an innovative retrofit solution for DHW production in a pilot building, located in Southern Italy. The proposed system, relying on thermal energy storage, decouples energy production and demand while also shaves demand peaks. It also offers a higher thermal efficiency and, at the same time, a greater user's autonomy through local storages installed in each dwelling.

This study is a part of the EU-funded H2020 innovation project entitled *e*-SAFE (Energy and seismic affordable renovation solutions) [30], dealing with solutions for the energy and seismic deep renovation of reinforced concrete (RC) framed buildings in the European countries. In terms of energy renovation, *e*-SAFE project appoints a central role to heat storage systems by developing innovative technologies that enable effective integration and communication in the DHW production, trying to overcome the most significant barriers faced by deep renovation in EU today. In the present study, firstly, features of the proposed retrofit solution are presented and thermal performance of the DHW production unit is experimentally investigated. Dynamic simulations are carried out to address subtle interactions in DHW network, in terms of the energy performance. Finally, the economic analysis of the proposed system is carried out. For both energy and economic analyses, the results yielded by the proposed model are compared with those of a typical centralised system for DHW production as a benchmark. The results of the present study are expected to provide a perspective for future studies regarding retrofit solutions for DHW system.

2. Description of DHW retrofit solution

The pilot building is a RC framed residential built in 1964 and located in Via Acquicella Porto, Catania, Italy (Lat: 37.30 North, Long: 15.07 East), characterised by warm and humid summer and moderately cold and wet winter seasons. It is a typical example of Mediterranean climate (Csa climate type), according to the Köppen-Geiger climate classification [31]. The pilot building has five stories with two residential units for each one, and a roughly rectangular footprint whose gross size is 24 × 9.5 m^2. Each apartment has a net floor area of 94 m^2, while the net height is 2.85 m. It belongs to a compound owned by the local public housing authority IACP Catania (Istituto Autonomo Case Popolari). Fig. 1 displays the climatic zone of pilot building under study as well as its current state.

The retrofit solution for DHW system proposes to remove current electrical boilers (decentralised) and to install a centralised PV-driven air source heat pump system relying on thermal energy storage to decouple energy production and demand. In order to make full profit of PV-based electricity production, the proposed solution appoints a central role to thermal energy storage: A first storage level is provided by a large centralised water tank which is equipped with a programmable control system to use the water tanks as a buffer and let the heat pump operate under desirable conditions. The second level of energy storage is provided by innovative slim and modular decentralised tanks, called hereafter *e*-TANKs, devoted to DHW production and storage, providing a higher thermal efficiency and, at the same time, a greater users autonomy through local storages installed in each dwelling. Schematic of *e*-TANKs circuit and apartments' arrangement by number in each floor with their corresponding number of occupants are illustrated in Fig. 2.

In this context, each apartment is equipped with a wall-mounted *e*-TANK system with an internal helical heat exchanger which is connected to a 2-pipe hot water network. The *e*-TANK system is installed on the lateral wall of the external balcony due to existing positions of main piping network, reducing construction works, minimising the installation costs and disturbance for the occupants. The proposed 2-pipe network can be utilised either for the charging of DHW storage tanks or for the heating purpose, which is beneficial in buildings with moderate heating demand. In both cases, the 2-pipe network can work at high temperature during charging periods for few hours a day, resulting in lower heat losses from the piping network and a lower consumption of circulating pumps, compared to traditional centralised DHW systems, where the recirculating network works 24 h at a relatively high temperature.

The *e*-TANK system consists of two main subsystems: The "storage tank" and the "hydronic module", designed and manufactured by PINK GmbH. Both components are connected and mounted on a steel frame, which then are fixed on existing walls. The slim storage tank has a

Fig. 1. The climatic zone and pilot building under study.

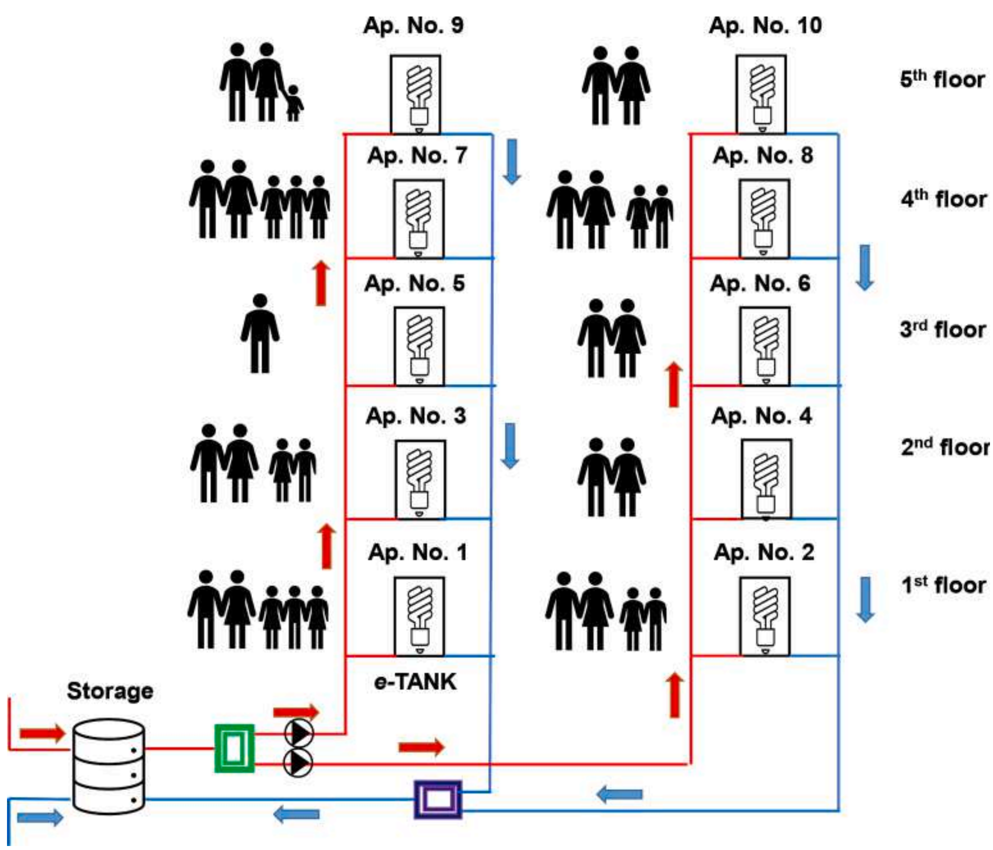

Fig. 2. Schematic of *e*-TANK circuit and arrangement of apartments in each floor by number with their corresponding number of occupants.

volume of 140 *l* and height of 1.72 m, made of stainless steel-1.4571 (V4A), as illustrated in Fig. 3 (a-d). The integrated coil heat exchanger, made of molybdenum-bearing austenitic stainless steel, has the heat transfer area of about 2.0 m^2 and a total length of coiled tube equal to 17.88 m. Since the heat exchanger reaches the top of the tank and it is operated in the counter flow configuration, the hot water can be provided much faster compared to typical hot water tanks, which typically have the heat exchanger positioned at the bottom. Furthermore, an internal sensor (Fig. 3 (c)) was integrated to the storage reaching the entire storage height with an inner diameter of 12 mm.

The hydronic unit and its characteristics are illustrated in Fig. 3 (d and e). The main features of hydronic unit include a control cabinet, the built-in auxiliary heater, the ultrasonic heat meter, the cold-water meter, the ultrasonic flow meter, 3-way diverter valve, and electrical ON/OFF actuator. The control cabinet includes a PLC (programmable logic controller) system, in which the control and monitoring activities can be realised. The built-in auxiliary heater with 1.5 kW power (upper left part of Fig. 3 (c and e)), screwed into the tank via 1 ½"coupling, consists of three U-shaped elements fitted in a brass nipple. The auxiliary heater is equipped with an electromechanical temperature controller and a safety temperature limiter according to EN 14597 [32]. The main logic of integrating the auxiliary heater to *e*-TANK is to facilitate fulfilling certain regulations regarding *Legionella pneumophila*, such as EN 806–1 [33], by boosting the tank temperature through the optional

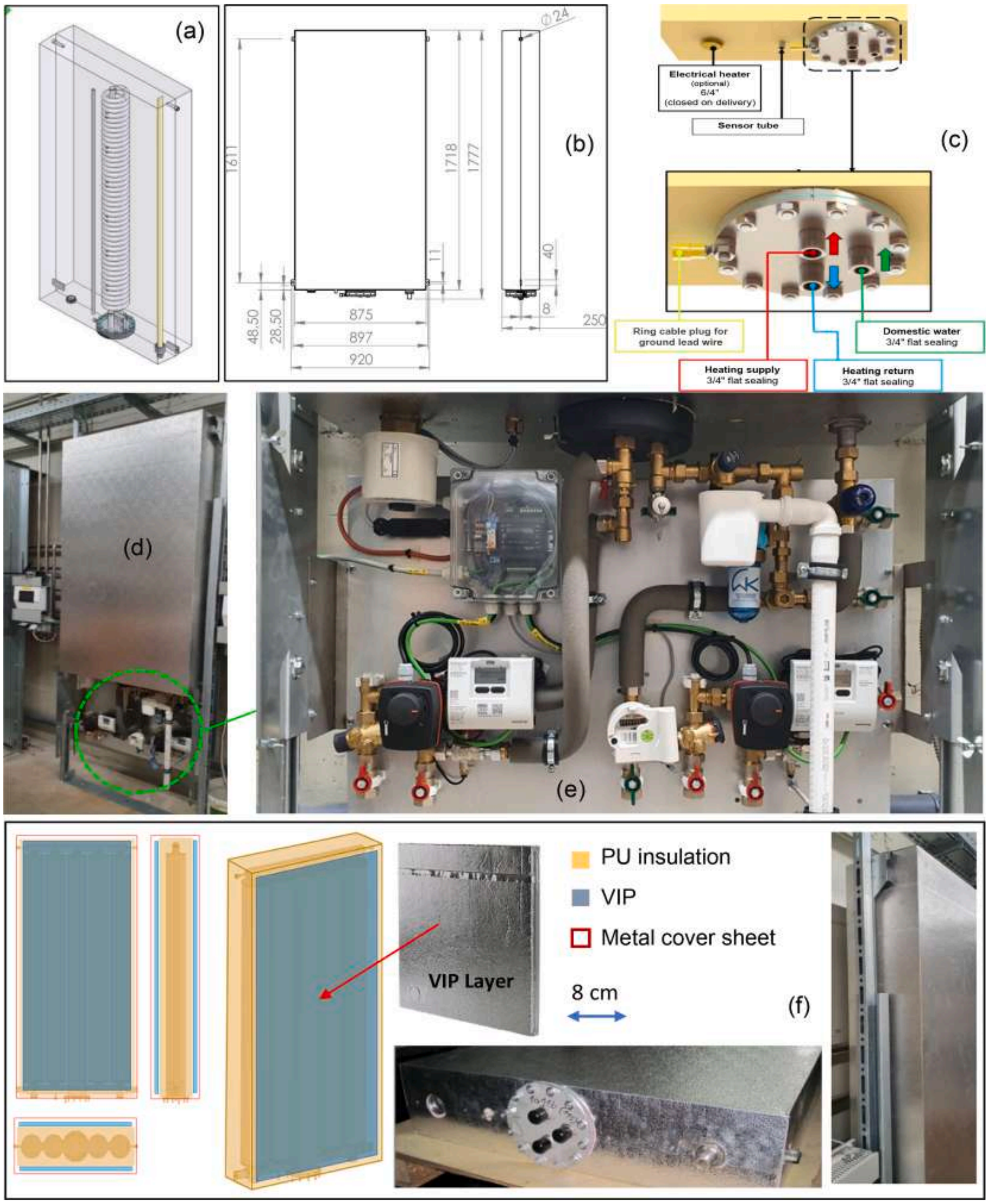

Fig. 3. Details and characteristics of the *e*-TANK system: Schematic of *e*-TANK (a), design and dimensions (b), connections to supply sources (c), prototype (d), details of the hydronic unit (e), and PU-foam insulation with additional VIPs (f).

electrical heater. Moreover, it allows heating up the water outside the central plant charging schedule and maintaining the tank temperature periodically higher by users' demand.

Regarding tank insulation, an 8 cm layer of vacuum insulation panel (VIP) were applied to the two largest surfaces of the tank, depicted in Fig. 3 (f), in addition to the conventional insulation by means of a PU foam. The experimental results indicates that utilised VIP layers, having the thermal conductivity of 0.007 W/(m.K), density of 200 kg/m^3 and loss coefficient of 0.32 W/(m^{2}K), reduces the stand-by thermal loss of *e*-TANK from 1.06 to 0.92 kWh/day.

To fulfil the legal obligations to cover the renewable energy system (RES) quota, the pilot building is equipped with 36 monocrystalline photovoltaic (PV) panels on rooftop, characterised by overall PV surface of 67 m^2 and total peak power of 13.5 kW. Electricity produced by solar modules can be either consumed instantaneously by the heat pump system or stored in a considered 20 kWh BESS (Battery Energy Storage System). Characteristics of the PV system are reported in Table 1.

Table 1
Technical features of the PV system.

Parameter	Value / Type
Slope	10°
Azimuth angle	9° West
Type of PV modules	Monocrystalline silicon
Efficiency in Standard Conditions (STC)	20.2%
Size of each PV module	1050 × 1770 × 35 mm
Number of PV modules	36
Overall PV surface	67 m^2
Peak Power (per PV module)	375 W
Peak Power (total)	13.5 kW

3. Dynamic simulations model

The energy performance of proposed DHW solution was examined by developing a dynamic simulation model established in TRNSYS software, which was coupled to a MATLAB code simulating the DHW consumption profile in each apartment. The dynamic simulations were carried out for duration of one year using a 1-min interval (time step). Moreover, the performance of proposed solution is compared to a common centralised system for DHW production with an identical generator system, i.e., PV-fed air-to-water heat pump system. In this context, two dynamic simulation models were established under equivalent simulation conditions and setups.

3.1. Generation of DHW profiles

To model the DHW consumption profile, a MATLAB code was established and linked to the TRNSYS model by introducing a NORMRND function. This function generates random samples from a normal (Gaussian) distribution through the mean and standard deviation parameters, allowing more realistic simulation of the daily DHW consumption for different daily time slots. The MATLAB code reads the simulation time and the number of occupants in each apartment from the TRNSYS model, and then at each time step, by considering the monthly factor and hourly profile, returns a value as a consumption to the TRNSYS.

The domestic hot water demands were regulated based on the number of occupants in each apartment, the seasonal (monthly) consumption factor, and the daily (hourly) consumption profile. According to the literature data, the mean daily DHW consumption for each occupant was considered equal to 45 *l* [34], varying slightly in each month, i.e. divided on the basis of cold and warm seasons [35]. In fact, the mean daily DHW consumption can be globally categorised in a wide range from 20 to 94 *l*/day/person, according to Annex 42 [36], depending on various influential factors. For the daily consumption profile, it was assumed that peaks of the daily consumption profile occur in the morning between 06:00 and 10:00 (45% of total daily consumption) as well as in evening between 18:00 and 22:00 (25% of total daily consumption) [37]. Moreover, for a given daily time slot, the adopted model simulates the hourly consumption for each apartment with slightly different pattern, satisfying mentioned peak time slots as well as the mean daily value.

3.2. The e-TANK solution

The technical layout of the proposed solution in Section 2 is presented in Fig. 4. The circuit fluid is supplied to each *e*-TANK with a flow rate of 300 kg/h through two circulating pump units (Type 743), i.e., each pump for five apartments located on each side of the building (Fig. 2), with the rated power and the maximum mass flow rate of 50 W and 1500 kg/h, respectively. The main storage tank was modelled by Type 4c component, with the volume of 1000 *l*, height of 2.4 m and the thermal loss coefficient of 0.40 W/m^{2}K, with a set-point temperature varying with the heat pump performance.

The heat pump is a reversible air-to-water system having a nominal 26.0 kW heating capacity and COP equal to 3.10 (A7/W45). The maximum water temperature supplied by the heat pump is equal to 65 °C for the outdoor temperature between 5 °C and 19 °C. Actual performance values were calculated based on the performance curve reported by the manufacturer taking the operating temperatures into account according to the approach suggested by Italian Standard [38].

The Type 534-Coiled was employed to simulate thermal performance of the *e*-TANK system, calibrated in charging and discharging process by experiments which is presented in Section 4.1. The *e*-TANK with volume of 140 *l* consists of two inlet and two outlet flow ports. To be more precise, inlet ports for Domestic Cold Water (DCW) and supply circuit fluid to heat exchanger, and outlet ports for discharged circuit fluid and delivery of DHW to users (yellow tube in Fig. 3(a)). According to the measured data, the thermal loss coefficient of *e*-TANK is equal to 0.56 W/m^{2}K. The heat generated by built-in auxiliary heater inside *e*-TANK was modelled by inserting a heat source input to specified nodes, according to its characteristics reported in Section 2. By utilising a thermostatic valve (Type 953), it was assumed that the draw-off temperature in baseline simulations is equal to 38 °C. However, the role of draw-off temperature on energetic result is also addressed, considering the draw-off temperature in the range between 38 and 42 °C.

An ON/OFF controller (Type 2) was employed for both central storage and *e*-TANKS to regulate the set-point temperatures in upper and lower limit of ± 2.5 °C. Moreover, the control logic of DHW system,

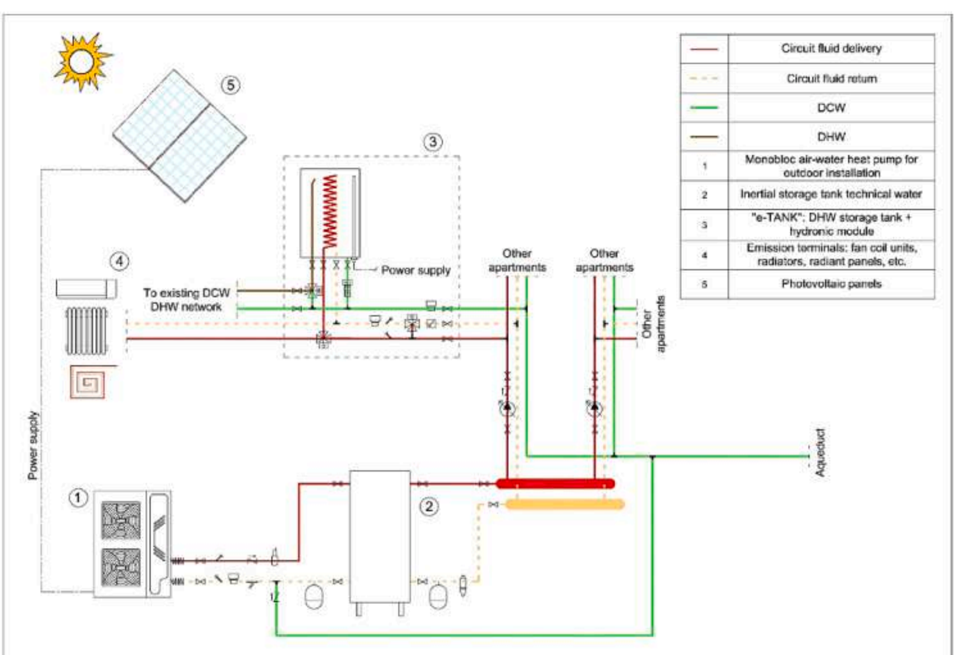

Fig. 4. Layout of the proposed retrofit solution for DHW production and heating.

including signal controls and activation timespans, was modelled by employing the equation/calculator unit, the timer Type 21, and the season scheduler Type 515. The weather data Type-15 was adopted for the external temperature as well as for the aqueduct temperature, connected to relevant components. The mean annual outdoor temperature and aqueduct (mains) temperature in the pilot building were equal to 17.8 and 19.2 °C, respectively. Furthermore, for the piping network, Type 31 model was employed for tubes and types 649 and 647 were adopted for mixing and diverting valves, respectively. The piping network consists of tubes with different internal diameters, varying from 16.2 mm to 51.4 mm, and an insulation thickness ranging from 19 mm to 33 mm, according to Italian regulation DPR 412/93 [39]. The total length of supply and return piping network is equal to 198.6 m.

The hourly electricity production from PV panels (Table 1) was calculated by using the EU tool called “PVGIS” [40], rendering the hourly global irradiation values (Wh/m^2) from the “SARAH 2″ database. Furthermore, the conversion factors for estimating the required primary energy as well as the CO_2 emission were adopted from the Italian Regional Legislative (DGR 967–1275/2015) [41].

3.3. Model of centralised system

The centralised system consists of an identical thermal generation system to that of the *e*-TANK scenario, namely, a mono-block air-to-water electrical heat pump system connected to PV panels and battery storage system (BESS). The circuit fluid (technical water) produced by the heat pump feeds the main storage via heat exchanger and after transferring heat to the aqueduct, the circuit fluid is discharged from the storage to the heat pump. The produced domestic hot water is distributed on– demand via piping network to users. Furthermore, as a general practice in customary centralised systems, the hot water is circulated by pump in the piping network to minimise the waiting time and to maintain the temperature as high as possible. The technical scheme of the centralised system is demonstrated in Fig. 5.

The piping network has a total length of 154 m for the supply and recirculation of DHW. It consists of tubes having an internal diameter ranging from 16.2 to 26.2 mm, with corresponding insulation thickness between 15 and 20 mm, based on Italian regulation DPR 412/93 [39]. The sizing of the main storage tank resulted in a required volume of 940 *l*. Considering the available storage tank sizes in the market, a storage with height of 2.2 m and volume of 1000 *l* was selected, with 14.0 m coiled tube length and coiled pitch of 0.045 m, having a thermal loss coefficient equal to 0.4 W/m^{2}K. In addition, the recirculating loop operates at mass flow rate of 280 kg/h, designed in accordance with technical considerations suggested in [42]. Regarding dynamic simulations, Types adopted in TRNSYS model for different components of the centralised system are identical to those adopted for *e*-TANK solution, described in Section 3.2, except for the main storage tank which is Type 534-Coiled.

3.4. Control strategy

Regarding the control logic, the circuit fluid is supplied to *e*-TANKs via the circulating pump in pre-defined activation time slots. A series of simulations were preliminary performed to optimise the charging scheme based on the DHW consumption profile. The details of the pertaining results can be found in [43]. The optimised daily charging scheme was a three-time charging between hours 06:00–09:00, 12:00–13:00, and 18:00–21:00, yielded by considering both the lower energy consumption and a better delivery of DHW to users at a higher temperature.

For the *e*-TANK solution, it was considered that the heat pump system works in accordance with the activation times of the circulating pump. The heat pump operates continuously from the start of the first available charge to the end of the last one, in order to minimise ON/OFF cycles of the heat pump. On the other hand, for the centralised system, the heat pump system operates 24 h. For both scenarios, when the temperature of main storage decreases to lower value than its set-point, the heat pump starts to feed the main storage. The set-point of main storage tank (T_{SP}) may vary with the outlet water temperature of heat pump (T_{Outlet}). Furthermore, the circulating pump is activated only when the temperature of main storage ($T_{Storage}$) be higher than set-point temperature of *e*-TANKS.

During the charging timespan of the circulating pump, if the temperature of any *e*-TANK drops below its set-point temperature (T^*_{SP}), due to either draw-off or thermal loss, the electronic valve inside the hydronic module immediately opens and charges the demanded *e*-TANK to reach the set-point temperature. Considering the curve of water

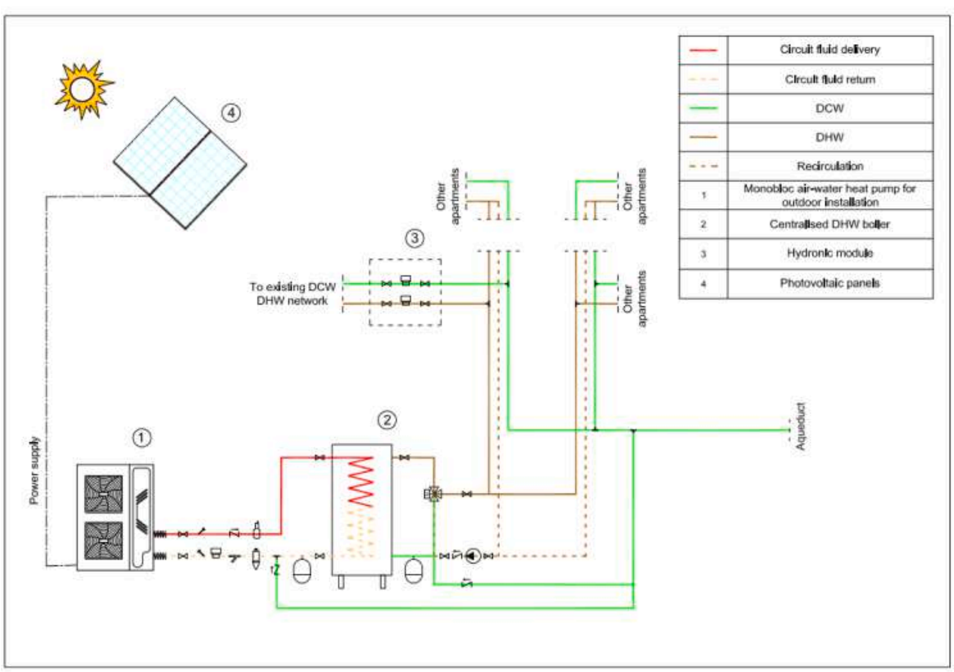

Fig. 5. Layout of the centralised system for DHW production.

temperature at the outlet of heat pump, the set-point temperature of e-TANK in cold seasons was regarded 50 °C while that in warm seasons was equal to 45 °C. If the temperature of e-TANK outside of the charging time slot drops below a pre-defined value by user (would occur after midnight in case of high demand), the built-in auxiliary heater is activated. The pre-defined temperature for activating the auxiliary electrical heater in simulations was considered equal to 40 °C. It is also noticeable that the "anti-legionella" treatment by auxiliary electrical heater was not considered in dynamic simulation due to the diversity of regulations. Details of the control strategies adopted for each component are reported in Table2.

4. Results and discussions

4.1. Experimental results and model calibration

As the main component for the proposed DHW solution, the experimental investigation on the performance of e-TANK system were carried out. The measured data was also utilised for the calibration of established numerical model for dynamic simulations of proposed DHW system. Experimental stratification of the e-TANK system during charging and discharging processes were examined for charging period of 30 min and discharging period of 10 min. An infrared thermal camera with accuracy of ± 1 °C (or ± 1%) and resolution of 640 × 512 pixels was utilised. The heat exchanger of e-TANK was charged with supply temperature of 65 °C at mass flow rate of 300 kg/h. Fig. 6 illustrates the temperature stratification for both charging and discharging processes in four picture frames.

Fig. 6 shows that, during 20 min of charging process, the level of temperature stratification ranges between 30 and 50 °C. After 30 min charging, it can be observed that only few layers at the bottom of the tank remain below 50 °C. The stratification also remains very stable during the discharging process in which the entire volume of the storage tank (140 *l*) is emptied within just 10 min. The figure demonstrates that despite the high withdrawal quantity, there is no mixing within the storage tank and therefore the entire storage volume is available at its maximum temperature.

Table 2
Details of the adopted control strategies.

Control level	Component	e-TANK solution	Centralised system
1	Heat pump	Operating time: 06:00–21:00 60 °C < T_{Outlet} < 65 °C.	Operating time: 24 h S 60 °C < T_{Outlet} < 65 °C.
2	Main storage	$T_{SP} = T_{Outlet} - 5.0$ °C (±2.5 °C); Charging condition: $T_{Storage} < T_{SP}$	$T_{SP} = T_{Outlet} - 7.5$ °C (±2.5 °C) Charging condition: $T_{Storage} < T_{SP}$.
3	Circulating pump (Via diverting/ mixing valves)	Charging time slots: 06–09, 12–13, 18–21. Conditions of pump activation: 1- Being in timespan of charging 2- $T_{Storage} > T^*_{SP}$ 3- $T_{e\text{-}TANK} < T^*_{SP}$	Operating time: 24 h; Supply conditions: Users' draw-off.
4	e-TANKs	In available charging timespans: –For $T_{Outlet} = 65$ °C (cold seasons); $T^*_{SP} = 50$ °C (±2.5 °C). –For $T_{Outlet} = 60$ °C (warm seasons); $T^*_{SP} = 45$ °C (±2.5 °C). Outside of the charging period: Activation of built-in auxiliary heater when $T^*_{SP} < 40$ °C (users' optional).	–

The nodal temperature stratification inside the e-TANK was measured for charging process by means of a sensor tube with internal diameter of 12 mm and a height equal to that of the tank with accuracy of ± 0.1 °C. Four nodal temperatures were regarded to be measured where the height of the highest one, namely node1, is identical to the height of DHW outlet port (to user) and the lowest one is node 4. The charging process was performed at flow rate of 300 kg/h and supply temperature of 45 °C. Fig. 7 compares the experimental and numerical time evolution of e-TANK's nodal temperatures in charging period of 60 min. Graphs of temperature stratification indicate that the temperature of DHW at outlet port reaches its asymptotic value in charging process, i.e., the maximum temperature, after about 40 min. The figure shows a good agreement between measured and numerical results. The root-mean-square-deviation (RMSD) of the simulated DHW profile from experimental was evaluated by using following equation:

$$RMSD = \sqrt{\frac{\sum_{i=1}^{N}\left(\left[T_{Exp}\right]_i - \left[T_{Num}\right]_i\right)^2}{N}} \tag{1}$$

and the RMSD of numerical DHW profile from measured ones is equal to 0.4 °C.

Fig. 8 compares the discharge volume of e-TANK for different supply temperatures, yielded by both experiments and simulations. A three-way thermostatic mixing valve was connected to the outlet port of e-TANK to maintain the draw-off water temperature at 40 °C, whereby the hot water is tempered with the cold water at 14 °C. The figure shows that the discharge volume is linearly an increasing function of the tank temperature. Elaboration of the results indicates that a 1.0 °C increase in storage temperature enhances 5.4 *l* on average the discharge volume of hot water (at 40 °C). The maximum discrepancy between numerical and experimental results obtained for discharged volume is equal to1.4% for $T_{e\text{-TANK}} = 60$ °C, corresponding to 3.4 *l*.

Similarly, Table 3 compares the experimental and numerical discharge capacity of e-TANK system for three different storage temperatures, namely, 45, 55 and 65 °C. The results show that, by 10 °C increasing tank temperature, the discharge capacity of e-TANK augmented on average 2.5 kWh. A comparison between simulated and experimental discharge capacity implies a discrepancy below 1.0% for all temperature levels of e-TANK.

4.2. Energy performance of DHW systems

The total daily consumption of DHW in pilot building, namely consumption of 32 occupants, is illustrated in Fig. 9 for a typical day in each season. The total daily consumption profile indicates that the highest hourly consumption occurs in the winter day (15 January) reaching 240 L, whereas, for the summer day (01 August), it is equal to188 litres. Fig. 9 shows that, regardless of the season, there are two peak timespans for DHW demand; first and the greater one is in the morning period, i.e., between 06:00 and 10:00, and another one in the evening, i.e., between 18:00 and 22:00. On the other hand, the lowest DHW demand is in the timespan between 00:00 and 06:00. According to Fig. 9, the mean daily consumptions per person in15 January, 20 April, 01 August, and 05 October is equal to 48.78, 46.15, 38.67, and 44.25 L, respectively.

Fig. 10 demonstrates the DHW consumption profile by apartment in various daily time slots of a typical winter day. A comparison between profiles of DHW consumption implies that each apartment has a different consumption pattern. This trend is generated thanks to the developed MATLAB code taking into account the number of occupants, monthly variation factor, and specified time slots in which the DHW is demanded. The developed code for the DHW consumption profile

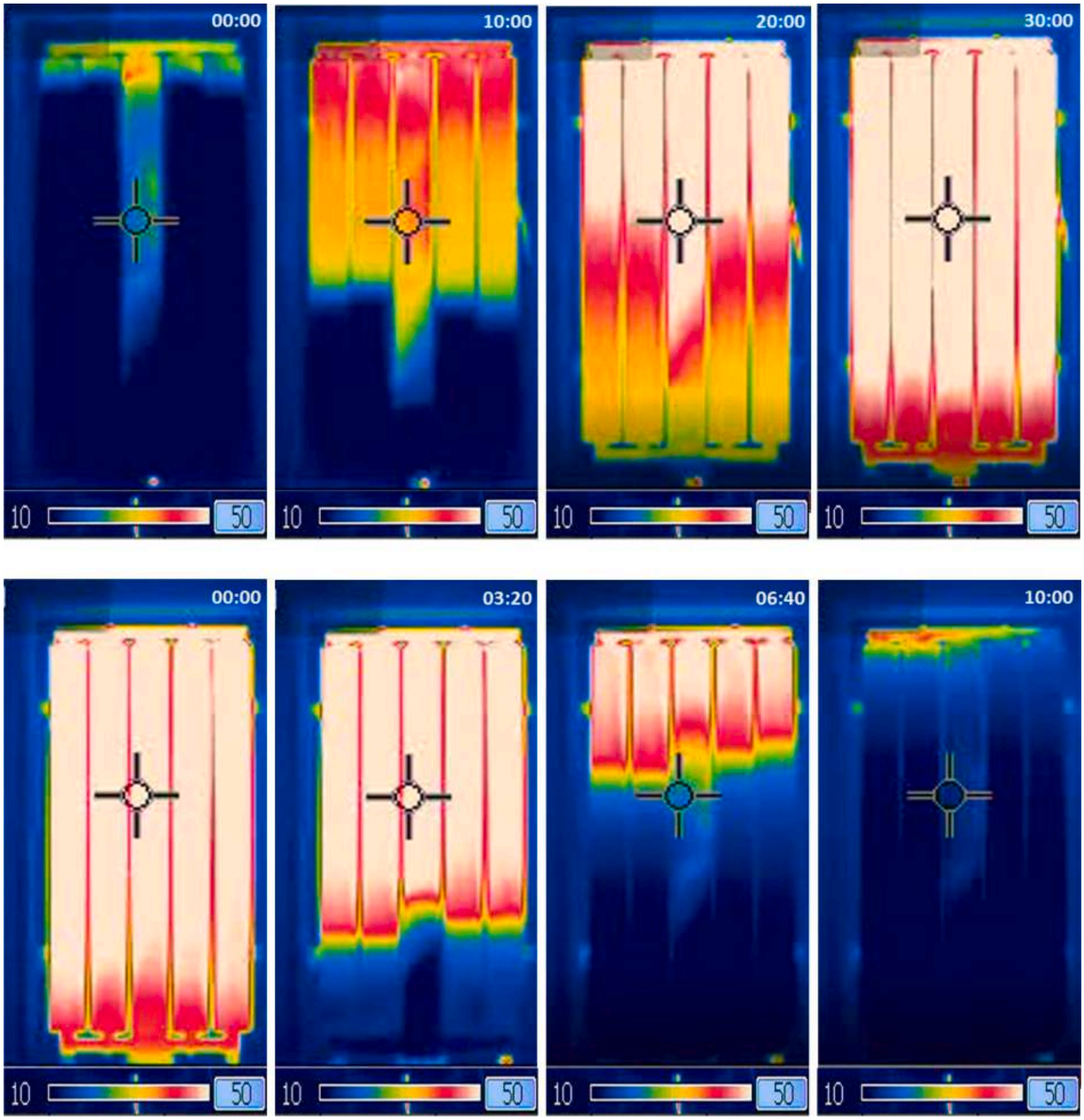

Fig. 6. Stratification of the *e*-TANK during charging period of 30 min and discharging period of 10 min.

renders a random value for each time slot in a predefined deviation threshold even for an identical number of residents and season. For example, while apartments No.1 and No.7 have the same number of occupants, the figure evidently shows a different consumption pattern in the same day. Nonetheless, it should be noted that the mean annual consumption for both apartments (and for others) is equal to 45 *l*/person/day. Moreover, it is noticeable from Fig. 10 that the peak consumption would occur in different hours for each apartment although they are all in the regarded time slots, e.g., 06:00–10:00.

Figs. 11 and 12 show the temperature variation in the outlet of main storage and in the temperature of hot water at draw-off points in a typical winter day, for centralised system and *e*-TANK solution, respectively. Two apartments from each side of the building (Fig. 2) with different number of occupants were selected, namely, No. 7 with five occupants and No.10 with two occupants. Graphs of Fig. 11 show that the temperature variation in hot water at drew-off points is a direct function of variation in the outlet temperature of main storage. Moreover, it indicates that the return temperature of recirculating network at inlet of storage is between 2.8 and 3.1 °C lower than that at outlet of storage (supply temperature), due to the thermal loss of piping network. The centralised system shows up to 1.7 °C temperature difference between two apartments at drew-off points, which can be explained by a longer distance of apartment No. 10 from generation source, with respect to apartment No.7.

On the other hand, Fig. 12 demonstrates that the *e*-TANK system maintains the temperature profiles for both apartments in the predefined set-point, i.e., 50 °C (±2.5 °C). However, it shows that the temperature profile in this system is affected by number of occupants, namely, the level of consumption, which is negligible in the centralised scheme. In this regard, it can be observed that, for apartment No. 7 (five occupants), the slope of temperature variation is steeper, and the number of peaks is higher, compared to apartment No. 10 (two occupants).

A comparison between two systems Implies that the main storage in centralised system requires a higher number of peaks, i.e., to be charged by the heat pump, to maintain the defined set-point temperature. In

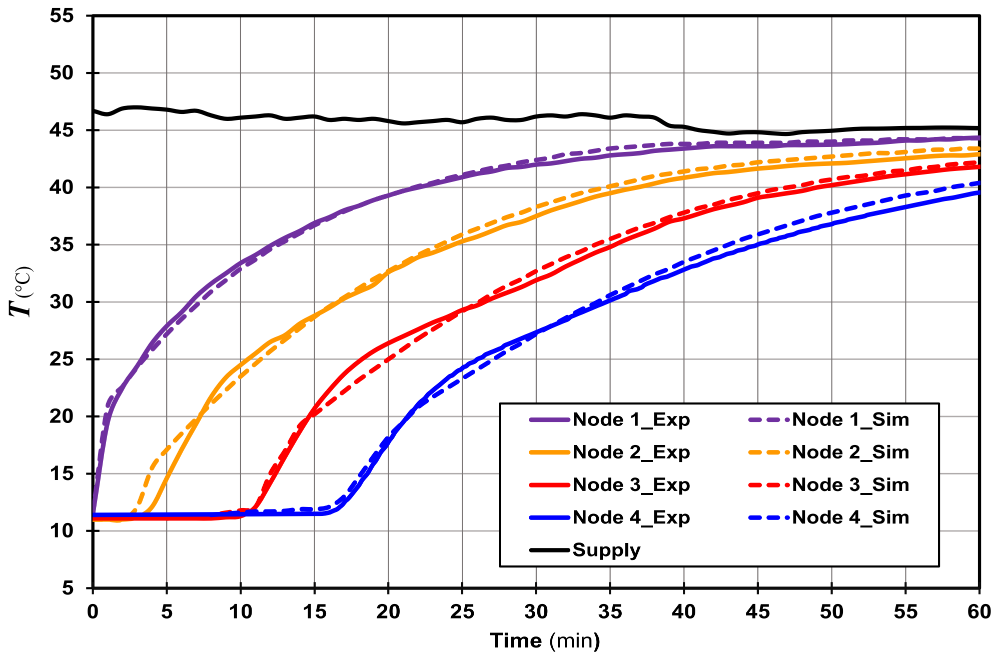

Fig. 7. Time evolution of *e*-TANK's nodal temperatures: Experiments vs. simulation.

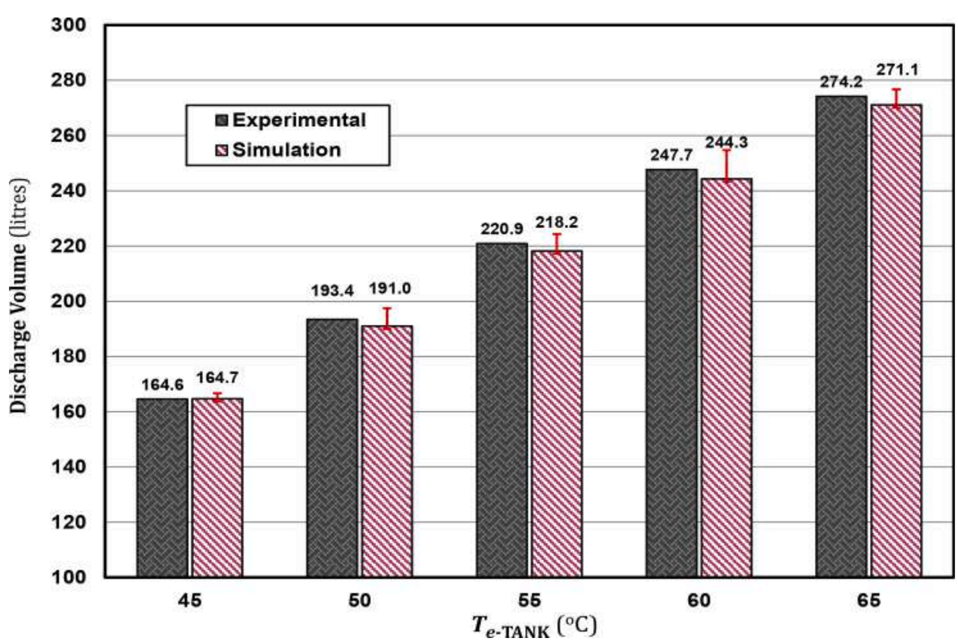

Fig. 8. Discharge volume of *e*-TANK at different temperatures: Experiments vs. simulations.

Table 3
Comparison between measured and simulated discharge capacity of *e*-TANK.

$T_{Storage}$	Discharge capacity	(kWh)	Discrepancy
(°C)	Experimental	Simulation	(%)
45	7.70	7.64	0.91
55	10.20	10.14	0.52
65	12.70	12.62	0.73

addition, for the given set-point temperatures of the main storage, the centralised system delivers the DHW at higher temperature, compared to *e*-TANK system. Nevertheless, it is noteworthy that the *e*-TANK solution provides a higher flexibility for delivery of hot water at desired temperature as well as a higher users' autonomy in heating up the tank over pre-defined set-point. The latter can be realised by activating the built-in auxiliary heater in this system.

To highlight energy performance of the proposed system in the pilot building, Fig. 13 compares the total monthly electrical energy consumption in three systems for production of the demanded DHW: *e*-TANK solution, centralised system, and existing decentralised system. The existing DHW system in pilot building is a cylindrical boiler heated by a 2 kW electrical resistance, installed in each apartment. In order to have a logical comparison between energy performance in previous and proposed ones, the set-point temperature, insulation characteristics and volume of tank in existing system were considered identical to those of the *e*-TANK system.

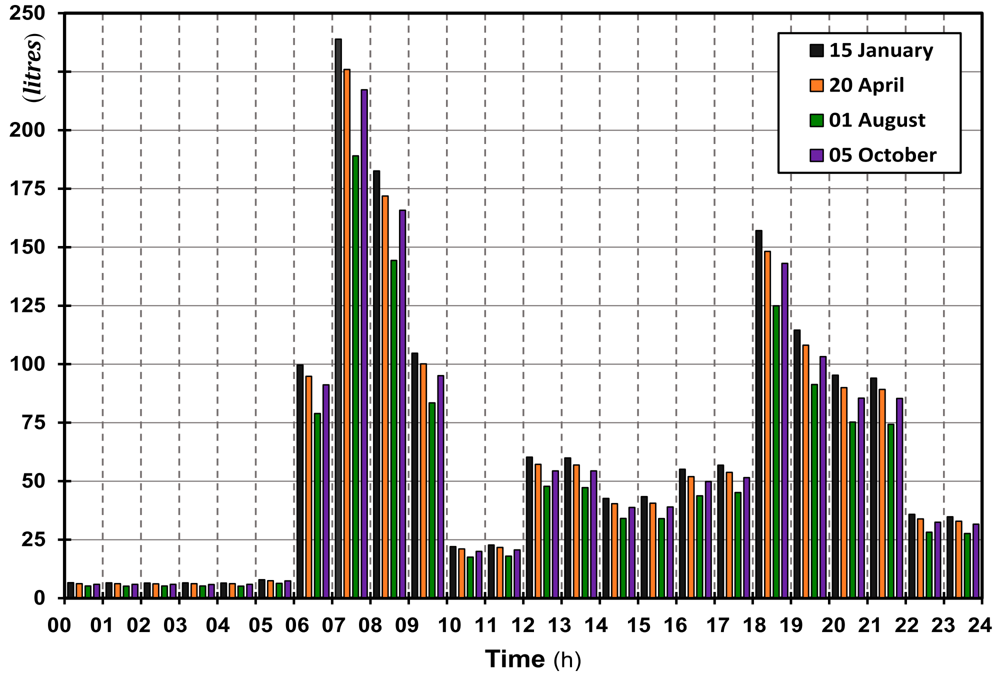

Fig. 9. Total daily consumption of DHW in pilot building for four typical days in each season.

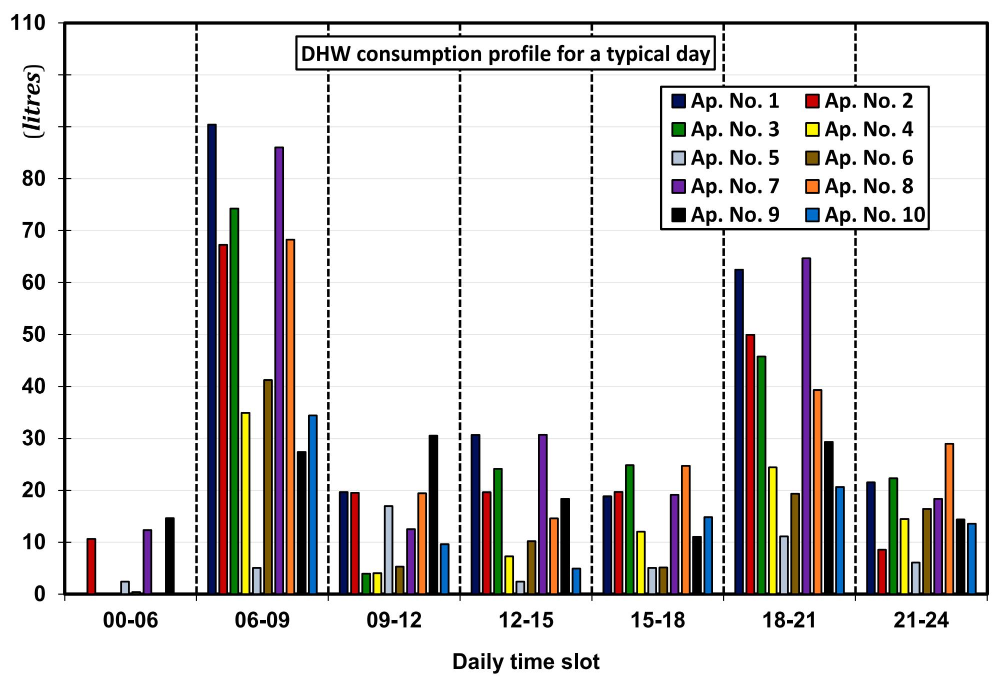

Fig. 10. Profile of DHW consumption by apartment in different daily time slots of a typical winter day.

The monthly required energy in all scenarios shows a parabolic trend with the minimum and maximum energy consumptions in August and January, respectively. This trend can be mainly justified by three synergetic factors: (*i*) A rather lower consumption level of hot water in warm months. (*ii*) A lower thermal loss from tanks and piping network in warm months. (*iii*) A lower set-point temperature for DHW production in summer. The figure indicates that monthly energy consumption of existing system can reach more than twice of that in either centralised or *e*-TANK systems. The highest ratio can be observed in August, in which the required electrical energy in decentralised (existing) system is 3.2 and 2.5 times greater than that in *e*-TANK and centralised ones, respectively. A comparison between two retrofit solutions implies that the *e*-TANK solution, on a monthly average, requires 51.2 kWh less electrical energy, compared to the centralise system, which requires monthly 550.4 kWh.

To better realise the composition of energetic data in each system, Fig. 14 illustrates the annual electrical energy consumption by the heat pump and circulating pump units, the total electrical energy consumption by whole-system, the required thermal energy produced by the heat pump, and the total thermal loss by storages and distribution network. Fig. 14 shows that the *e*-TANK system has the lowest energy consumption among all systems, and that existing system consumes annually

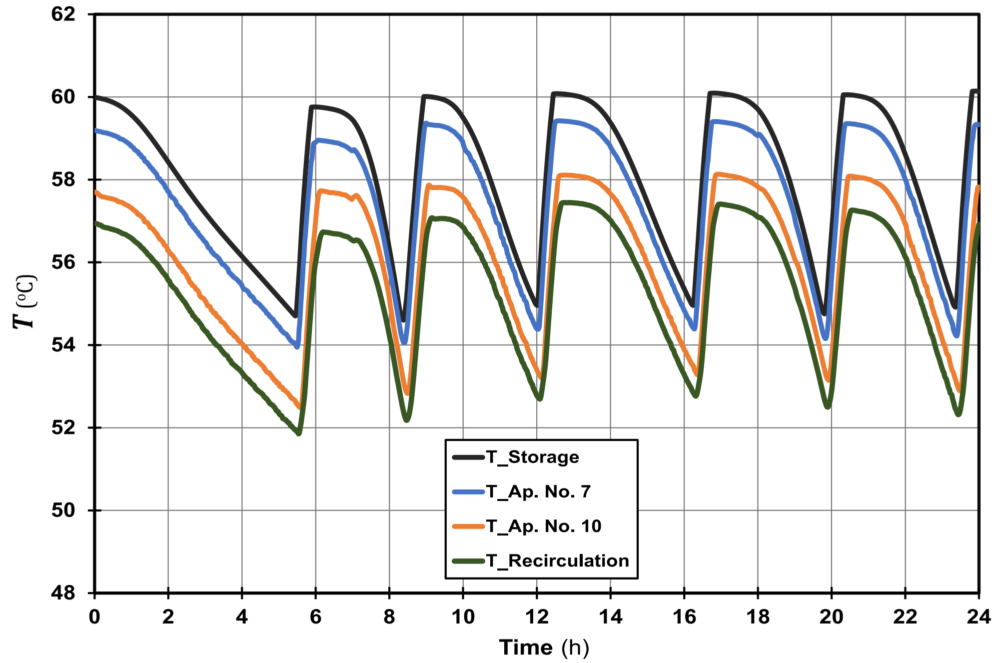

Fig. 11. Temperature profile in centralised system for a typical day: Variation of temperature at the outlet of main storage, at draw-off points in two selected apartments, and in recirculating network (at storage inlet).

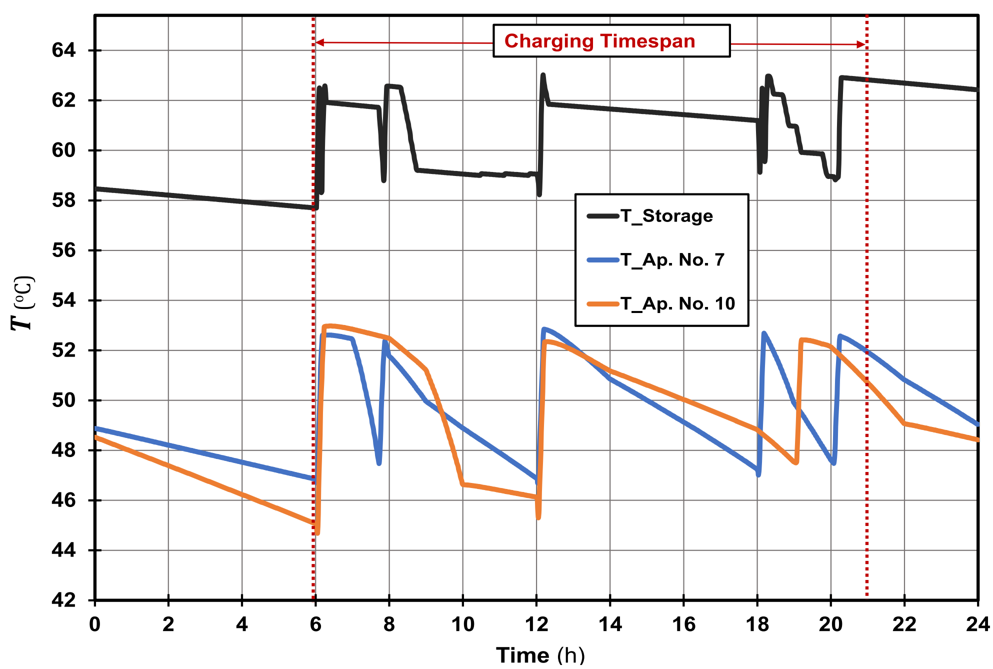

Fig. 12. Temperature profile in *e*-TANK solution for a typical day: Variation of temperature at the outlet of main storage, at draw-off points in two selected apartments (at *e*-TANK outlet).

7,207 and 6,706 kWh more electrical energy than *e*-TANK and centralised system, respectively. It can be also observed that the centralised system requires annually almost 11 times larger electrical energy for circulating pump than the *e*-TANK solution, which is due to 24 h recirculation of hot water.

A comparison between results obtained by retrofit solutions implies that annual consumption of the heat pump in centralised system is slightly higher than *e*-TANK solution, whereas the total thermal loss in the centralised system is more than 19% larger than that in *e*-TANK. It is not surprising to observe that thermal loss from existing system is the lowest among others, which can be explained by not having thermal loss from the piping network and the main storage. In this context, Table 4 compares two indices to reflect better the thermal loss from each component of DHW system, given by Eqs. (2) and (3): The ratio of total thermal loss ($E_{loss\text{-}tot}$) to the produced thermal energy ($E_{th\text{-}tot}$) in percentage for each scenario, denoted by ε_{loss}, and the share of thermal loss by each component in percentage, denoted by f_i.

$$\varepsilon_{loss} = \frac{E_{loss-tot}}{E_{th-tot}} \times 100 \tag{2}$$

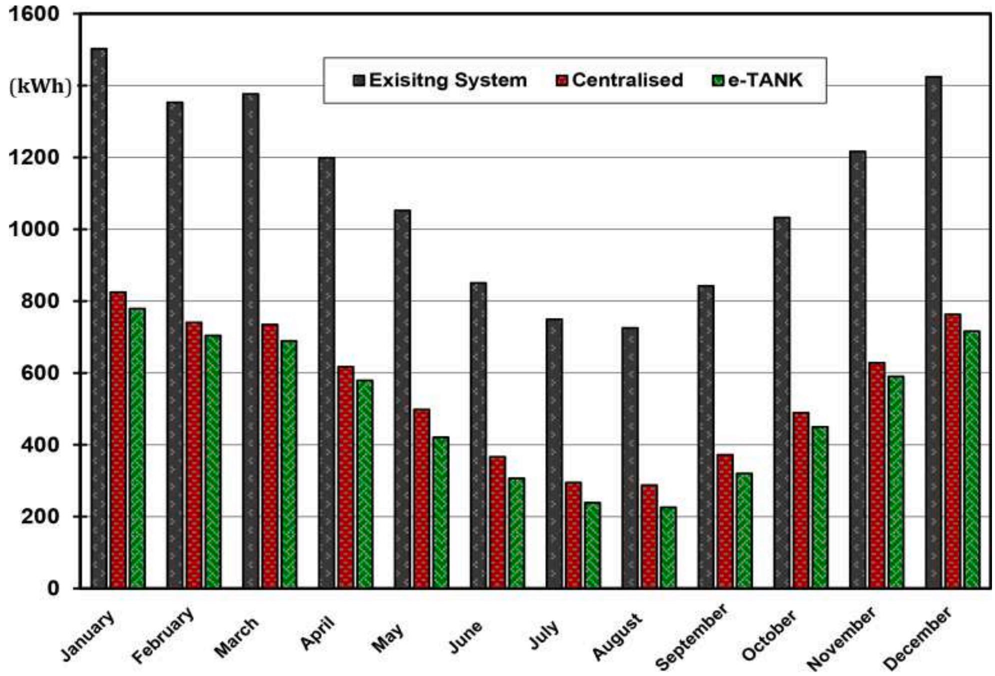

Fig. 13. Monthly total electrical energy required to produce DHW in three systems.

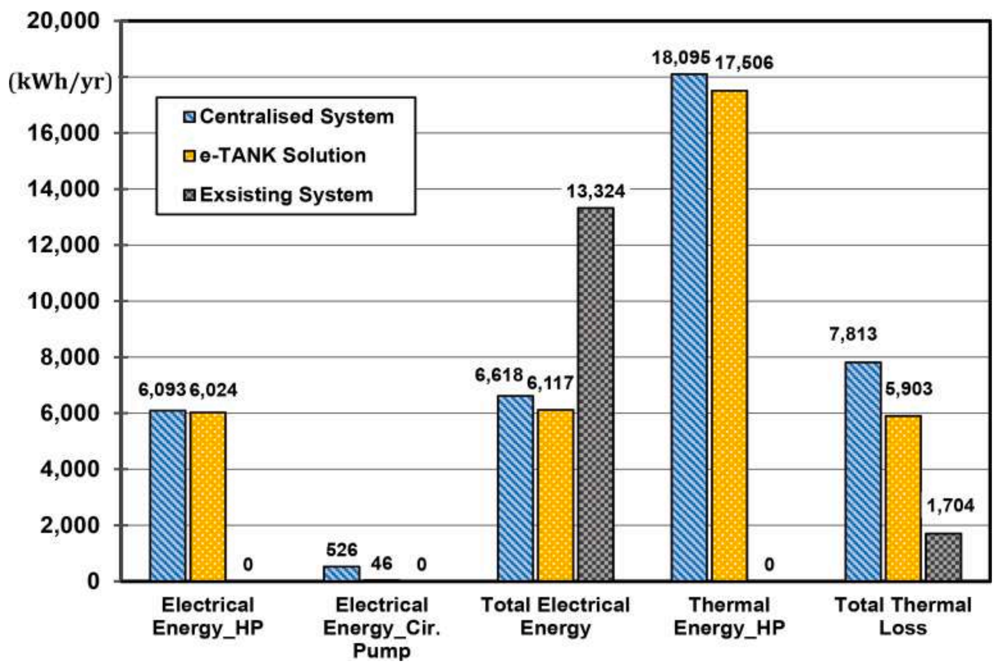

Fig. 14. Composition of annual energetic data for the DHW production in three different scenarios.

Table 4
Comparison between the ratio of thermal loss to produced thermal energy (ε_{loss}) and the fraction of thermal loss from each component (f) for three systems.

Scenario	$E_{loss\text{-}tot}$ (kWh)	ε_{loss} (%)	$f_{Storage}$ (%)	f_{Tanks} (%)	f_{Tubes} (%)
e-TANK	5,903	33.7	11.5	30.2	58.3
Centralised	7,813	43.2	10.2	–	89.8
Existing system	1,704	12.8	–	100.0	–

$$f_i = \frac{E_{loss-i}}{E_{loss-tot}} \times 100 \tag{3}$$

The results reported in Table 4 shows that ε_{loss} in *e*-TANK system is equal to 33.7% while in centralised system it reaches over 43%. The table also shows that the loss fraction from piping network is 31.5% higher in centralised system, compared to *e*-TANK. Moreover, it can be observed that 30.2% of total loss in *e*-TANK system is due to decentralised tanks installed in each dwelling, which is 18.7% higher than the thermal loss from the main storage.

Fig. 15 compares the amount of required daily energy for DHW production per household in different countries [34,36,44] with the

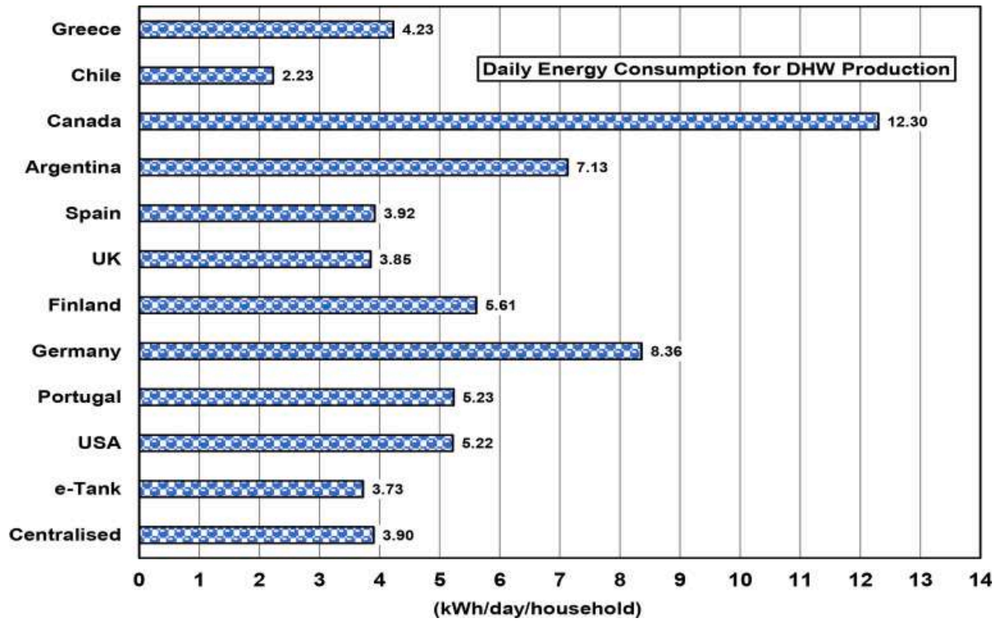

Fig. 15. Comparison of the daily energy consumption for DHW production per household in the present study with available literature data for different countries [34,36,44].

results yielded in the present study for centralised system and *e*-TANK solution. Daily hot water consumption per household by country, according to the report from Annex 42 [36], was calculated based on a 45 °C temperature rise for an average household of 2.5 occupants. The figure shows a significant difference in the daily required energy for DHW production in different countries. Indeed, this variety can be explained by striking dependency of the required energy to the mean daily hot water consumption as well as the time-dependency of DHW profile. The figure indicates that the daily energy consumption per household in *e*-TANK system is equal to 3.73 kWh while this amount for centralised system reaches 3.90 kWh. According to Fig. 15, the closest countries to those cases in pilot building, in terms of daily energy consumption for DHW production, are the UK and Spain with 3.85 and 3.92 kWh/day/household, respectively. On the other hand, the required energy for daily DHW production in Canada, Germany and Argentina are by far higher than scenarios in the present study. In addition, the case of Chile represents the lowest level of required daily energy for DHW production. However, it is noticeable that the hot water consumption due to shower has not been included in the report for the case of Chile, according to [44].

Elaborations of the obtained results for both scenarios imply the significant impacts of the draw-off temperature on the energy consumption of the heat pump. In this regards, Fig. 16 compares the hourly energy consumption of the heat pump in both scenarios in a typical winter day for two draw-off temperatures, namely, 38 °C and 40 °C. The figure evidently shows that an increase in draw-off temperature raises the peak of heat pump consumption for both cases; a two-degree increase in the draw-off temperature raises the energy consumption of heat pump 5.4% and 6.9%, for the centralised system and *e*-TANK solution, respectively. This issue on the annual basis can be better reflected by the results reported in Table 5, which compares the effect of draw-off temperature on the annual energy consumed by the heat pump system, annual total thermal loss, and corresponding annual emission of CO_2 per user. The table indicates that, a degree increase in draw-off temperature leads to annual 196 and 213 kWh increase on average in the heat pump energy consumption, for the centralised and *e*-TANK systems, respectively. Moreover, in terms of the total energy consumption by each system, table reports a corresponding 2.65 and 2.89 kg increment on average in the CO_2 emission per person for a degree increase in the draw-off temperature, respectively, for the centralised and *e*-TANK system.

To shed light on the role of proposed PV-BESS system for supplying electrical energy, Fig. 17 compares the annual required primary energy (PE) and the share of renewable energy source (RES) under different electricity supply scenarios. These supply scenarios are as follows: the total electrical energy required for DHW system is supplied by the external grid, by utilising the PV system (without battery), and by adopting the PV system in conjunction with the battery energy storage system (BESS). The figure shows that the total primary energy for the external grid case is 25.9 MWh in *e*-TANK solution, of which 54.6% is renewable, while this amount reaches over 27.0 MWh in the case of centralised system, with RES quota of 52.1 %. Fig. 17 shows that integrating the PV panels into the DHW system reduces the amount of annual primary energy around 3.0 MWh for both cases, with corresponding RES quota of 63.8% (centralised) and 67.1% (*e*-TANK). Finally, for the proposed PV + BESS system in pilot building, the total annual primary energy is further reduced (to 18.8 MWh) with renewable quota of 82.6%, which is 298 kWh lower than that in the centralised system.

4.3. Economic assessment of e-TANK solution

The economic analysis of the proposed system is examined and the obtained results are compared with those of a typical centralised system. Since the proposed retrofit solution via a 2-pipe network in the pilot building stands also for the heating system, the economic analysis encompasses both heating and DHW networks in both scenarios. In this regard, capital expenditures of the whole-system consist of purchase (C_p) and installation (C_i) costs, and is expressed by [45]:

$$C_S = C_p + C_i \tag{4}$$

and operating costs of the system can be calculated by:

$$C_{opr} = C_e + C_w + C_m \tag{5}$$

where C_e, C_w and C_m stand for the total electricity cost, consumed tap water price and maintenance costs, respectively. In the present study, capital expenditures for the purchase (C_p) and installation (C_i) of systems were investigated according to *e*-SAFE project documentations [30], provided by different partners and contractors. Table 6 compares the capital expenditures of system (C_s) by main components for both

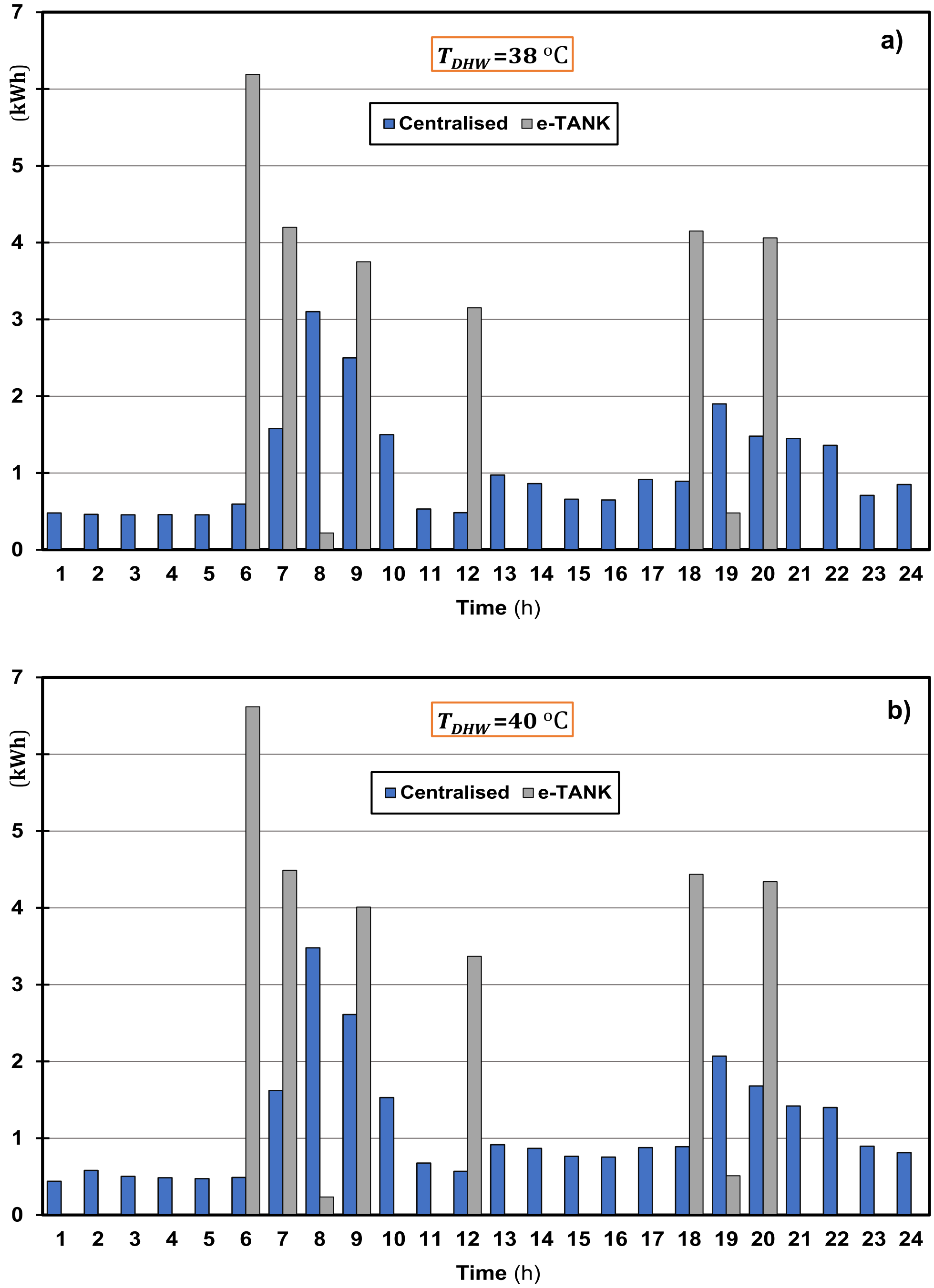

Fig. 16. Hourly electrical energy consumed by the heat pump system at two different draw-off temperatures, namely, 38 °C (a) and 40 °C (b): Centralised system vs. *e*-TANK solution.

Table 5
Impact of the draw-off temperature in two scenarios on the annual energy consumed by the heat pump system, total thermal loss, and corresponding emission of CO_2 per person.

	Centralised			*e*-TANK		
T_{DHW} (°C)	$E_{el\text{-}HP}$ (kWh)	$E_{loss\text{-}tot}$ (kWh)	CO_2 emission (kg/yr/prs)	$E_{el\text{-}HP}$ (kWh)	$E_{loss\text{-}tot}$ (kWh)	CO_2 emission (kg/yr/prs)
38	6,091	7,813	89.58	6,024	5,903	82.81
40	6,474	7,833	94.76	6,440	5,938	88.79
42	6,875	7,841	100.20	6,835	5,981	94.36

scenarios, including purchase and installation costs.

Table 6 shows a striking difference in the total cost of storages, distribution systems including piping network and connections, and required heat meters, which can be justified by different technical schemes and therefore different quantities of required components in each system. The results reported in Table 6 imply that the *e*-TANK solution, in terms of both mechanical and electrical systems, requires lower initial investments, i.e., up to 13.7%, compared to centralised one. However, the cost of regulation/control systems in *e*-TANK is higher since the *e*-TANK solution is basically a control-based system. It is also noteworthy to mention that this cost may differ to some extent in both systems since it is strikingly dependent to the level of adopted control strategy. A comparison between the amount of total initial expenditure

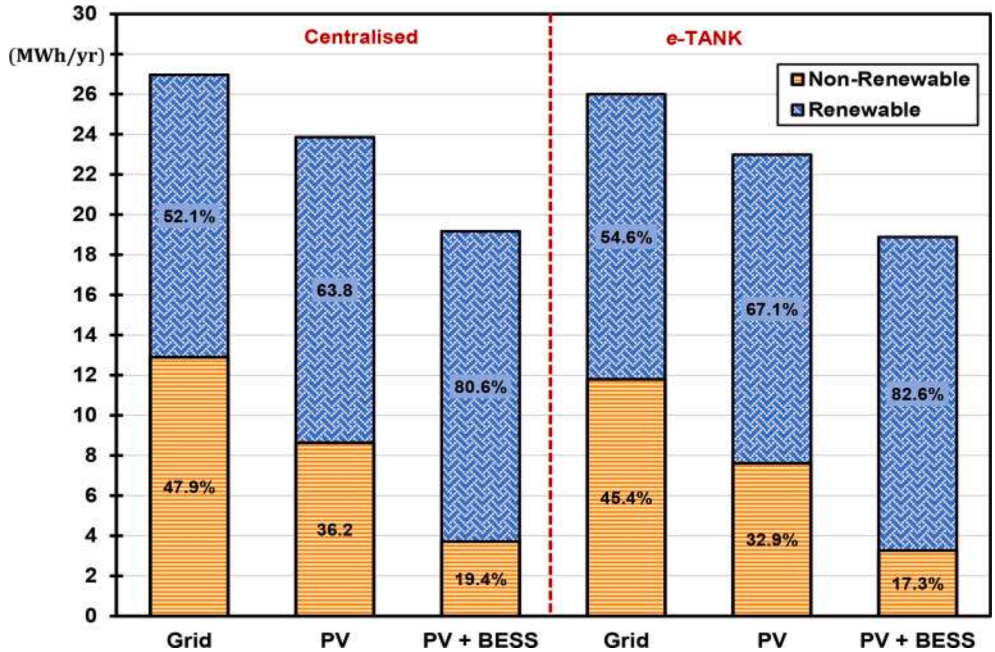

Fig. 17. Annual required primary energy as well as the share of renewable source for DHW production under different electricity supply scenarios: *e*-TANK solution vs. Centralised system.

Table 6
Details of components and their total cost, including purchasing and installation costs, for DHW and heating purpose: *e*-TANK vs. Centralised.

		e-TANK		Centralised		
No.	**Item**	**Quantity**	**Price (€)**	**Quantity**	**Price (€)**	**Comments**
1	Heat pump system	1	14,500.00	1	14,500.00	A2W EHP; 400 V-3–50 Hz, 26 kW (A7/W35); including concrete base and anti-vibration supports, covers and hydronic circuit connection.
2	Central storage tank	1	3,738.00	2	8,233.05	Stainless steel inertial storage with polyurethane insulation + AISI 316 stainless steel tank, fully insulated with spiral heat exchanger (centralised).
3	Technical cabinet	1	8,000.00	1	8,000.00	Construction of prefabricated metal cabinet (4 m × 2 m × 2 m) to protect the thermal plant.
4	Connections/ Valves	39	3,396.02	52	7,137.64	Including thermostatic valves, ball valves, elastic joints, flanges, check valves, safety valves, F-F connections, disconnectors, and three-way diverter valves.
5	Expansion vessel	2	494.29	3	592.94	welded expansion vessel for CE certified heating systems; steel body; SBR diaphragm.
6	Filters/ Separators	4	698.66	4	655.13	Including Y-type PN-16 impurity collectors and magnetic separators.
7	Piping network	–	12,498.40	–	18,633.20	Tubes and insulation according to DPR 412/93; total 471 m for centralised and 295 m for *e*-TANK (DHW + heating).
8	Heat meter	1	3,750.00	12	19,500.00	Direct heat meter for the heating and DHW services, regulation, and balancing.
9	Thermostats	10	705.60	10	705.60	Room programmable thermostats
10	Cold water counter	1	68.28	1	90.00	Dry dial; DN 50 mm (centralised) and DN 40 mm (*e*-TANK).
11	*e*-TANK storage	10	21,000.00	–	–	Decentralised hot water tanks with hydronic module and all necessary connections.
12	Circulating pump	2	3287.30	3	4930.95	−20 ÷ +120 °C; PN 10; IP 55, power supply 230/400 V.
13	Other equipment	12	1,757.63	5	983.72	Deaerator, polyphosphate dispenser with bypass (DN 25 mm), diaphragm pressure reducer, etc.
Sum	Mechanical plant	–	73,894.18	–	83,962.23	–
14	Electrical plant	–	13,300.95	–	15,113.20	–
15	Regulation/ Control systems		20,000.00		15,000.00	Regulation system for the control of heat pumps, circulating pumps, and valves by with BUS data transmission to/from thermal power plant and from/to local modules (*e*-TANK). Including data distribution lines, PLCs, electrical switches, temperature probes, etc.
Sum	Total		107,195.13		114,075.40	

shows that the centralised system requires about €7,000 more investment than the *e*-TANK solution.

To highlight better the composition of total expenses required for each system, Fig. 18 demonstrates capital expenditures for five main categories as well as their share from the overall cost in both scenarios. These categories include the thermal/generator system, distribution network, in-building (components/work inside apartments), electrical plant, and control/regulation systems. For both scenarios, the thermal plant with 46.1 and 35.7% has the largest share, for centralised and *e*-TANK systems, respectively. While the distribution network in the centralised system stands for the second largest share with 16.3%, in-building expenditures with 21.6% is the second most expensive category in the *e*-TANK solution with over €23,000, which is mainly due to purchase and installation of decentralised plug-and-play storage tanks.

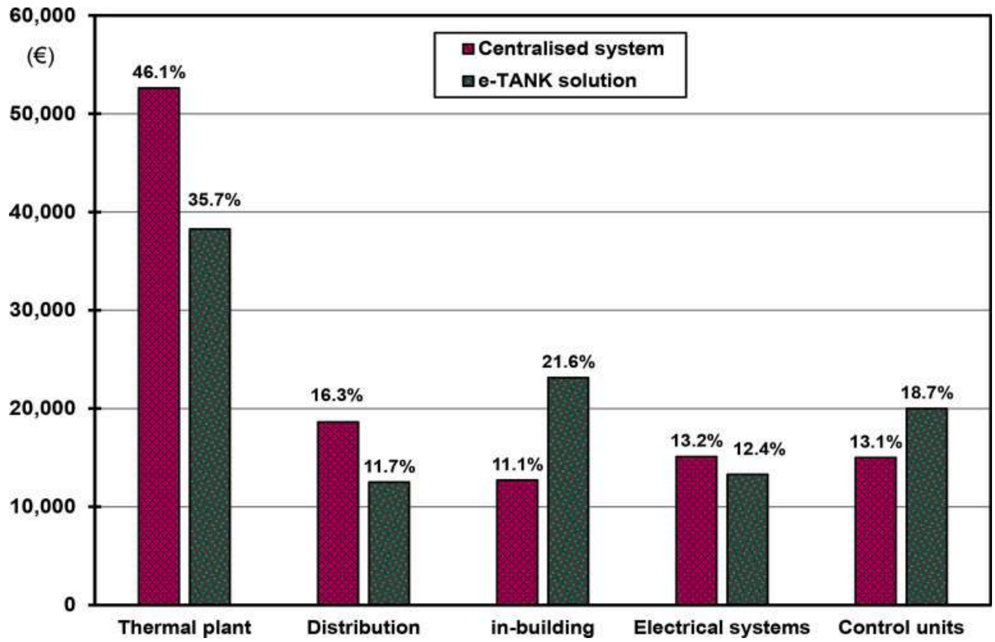

Fig. 18. The capital expenditure, including purchase and installation costs, for five main categories and their share from the total cost: *e*-TANK vs. Centralised system.

Moreover, Fig. 18 demonstrates a rather similar share of the electrical plants (around 13%) in both scenarios, with less than 1% discrepancy.

The Life Cycle Cost (*LCC*) of the system, the so-called cost of entire lifespan, which takes into account the initial investment (C_s) and operating costs (C_{opr}) incurred during the exploitation of the facility, was evaluated by the following equation [46]:

$$LCC = C_p + C_i + \sum_{t=1}^{n} \frac{C_e + C_w + C_m}{(1+r)^{t-1}} \quad (6)$$

where *r* is the discount rate and *t* is the number of years in use.

For calculations of the operating costs, the electricity and tap water price in the year 0 were estimated with average prices for Italy in 2023, according to [47,48]. Moreover, in order to obtain the electrical energy consumed for the heating purpose, the energy demand of the pilot building for space heating was simulated by means of EnergyPlus software, by setting the indoor temperature at 20 °C in the winter (heating) and considering a mean daily ventilation rate equal to 0.3 ACH, as suggested by the Italian standard [49]. The reference activation period of the heating system was considered from 1st December to 31st March. Technical characteristics of the pilot building including U-values, floor and wall assembly, thermal bridges, and infiltrations can be found in detail in [50]. In addition, for evaluation of operating costs, it was assumed that the required electricity for both systems is supplied by the grid and the maintenance costs were disregarded for both systems.

Table 7 reports relevant parameters for evaluation of the operating cost and compares the *LCC* values for a 20-year timespan at three different draw-off temperatures, namely 38, 40 and 42 °C. It shows that a degree increment in the draw-off temperature leads to a 0.4% increase on average in the total lifespan cost for both systems. The table reveals that, for a 20-year timespan, the *LCC* of *e*-TANK system can be up to 6.1% lower than that of centralised system, corresponding to around €8,300. Elaboration of the results also indicates that the difference between *LCC* graphs becomes larger over each year, which is due to a higher annual increase in operating costs of the centralised system compared to *e*-TANK solution, i.e., a higher electrical energy consumption in centralised system. Nonetheless, it is noteworthy to mention that centralised systems, in general, can be considered as more advantageous to reduce the investment and operating costs on a larger scale, namely in buildings with larger number of households/apartments, compared to decentralised solutions.

Table 7
Parameters related to operating costs and corresponding *LCC* for both scenarios at three different draw-off temperatures.

Parameter		Value	
The cost of purchasing electricity in the year 0		0.1744 €/kWh [47]	
The cost of purchasing tap water in the year 0		1.30 €/m^3 [48]	
The annual increase in electricity price		4% [44]	
The annual increase in tap water price		6% [44]	
Analysis period		20 years	
Discount rate		5% [10]	
Draw-off temperature (T_{DHW})	38 °C	40 °C	42 °C
LCC for *e*-TANK solution (€)	134,937.13	135,983.31	136,956.12
LCC for Centralised system (€)	143,204.69	144,107.91	145,060.36

5. Conclusions

In the present study, the techno-economic assessment of an innovative retrofit solution for production of domestic hot water (DHW) was accomplished. The proposed solution, aimed at enabling effective integration and communication in the DHW production, attempts to overcome the most significant barriers faced by the deep renovation of the DHW system. Firstly, thermal performance of the proposed system for DHW production was experimentally investigated. To identify subtle interactions in components of DHW system, dynamic simulations were carried out by establishing a coupled TRNSYS-MATLAB code, calibrated by measured data. The energy performance of the proposed retrofit solution was compared to those of the existing system in the pilot building as well to a typical centralised system as a benchmark solution. Finally, economic analysis of the *e*-TANK system was performed to address capital expenditures of the system, including purchasing and installation costs, as well as the life cycle cost (*LCC*).

The experimental results showed a desirable thermal performance for the proposed *e*-TANK system in both charging and discharging processes. The result obtained through dynamic simulations indicated that the *e*-TANK system reduces the annual energy consumption for DHW production more than 7,200 kWh, compared to the current DHW system. It was shown that a typical centralised system requires about 11 times higher electrical energy for the circulating pump than the *e*-TANK solution. The annual electricity consumption of the heat pump in centralised system was slightly larger than that in the *e*-TANK, whereas the total thermal loss in the centralised system was more than 19% larger. It was also revealed that the fraction of thermal loss from piping network is 31.5% higher for the centralised system.

Economic assessment of the proposed solution implied that this system, in terms of both mechanical and electrical components, requires lower initial investment (up to 13.7%) than a typical centralised system. However, the cost of control systems in *e*-TANK solution was higher since this system is basically a control-based-system. In addition, it was shown that for a 20-year timespan, the *LCC* of the proposed solution was 6.1% lower than that of a centralised system. Furthermore, it was turned out that applying the proposed PV-BESS system for electricity generation reduces 7.1 MWh/yr the required primary energy, compared to the case that the electricity is provided by the grid.

The techno-economic comparison between two systems in the pilot building under study as well as addressing the deep renovation limitations for both DHW and heating networks, including construction work, occupants' disturbance, and operational costs, indicate the privilege of the proposed retrofit solution for DHW system. The outcomes of the present study for the pilot building are expected to be extended to a significant portion of the existing European building stock. Indeed, future research in the framework of the *e*-SAFE project seeks to scale up the applicability of the proposed solution to a wider European context. Nevertheless, further analysis on possible technical issues as well as clarifications on the potential effectiveness of the proposed retrofit solution in different buildings under various characteristics and climatic conditions still needs to be addressed. In this context, the next phase of the present study will be devoted to the techno-economic evaluation of the proposed retrofit solution in other European pilot buildings with distinct characteristics.

CRediT authorship contribution statement

Aminhossein Jahanbin: Conceptualization, Methodology, Software, Validation, Formal analysis, Investigation, Visualization, Writing – original draft, Writing – review & editing. **Giovanni Semprini:** Conceptualization, Supervision, Visualization, Resources, Funding acquisition, Writing – review & editing. **Maurizio Goni:** Methodology, Software, Investigation.

Declaration of Competing Interest

The authors declare that they have no known competing financial interests or personal relationships that could have appeared to influence the work reported in this paper.

Data availability

Data will be made available on request.

Acknowledgments

The present study was carried out in the framework of the "Energy and seismic affordable renovation solutions" (*e*-SAFE) project, which received funding from the European Union's Horizon 2020 research and innovation programme under grant agreement No. 893135.

References

[1] Anisimova N. The capability to reduce primary energy demand in EU housing. Energ Buildings 2011;43(10):2747–51.
[2] European Parliament. Proposal for a DIRECTIVE OF THE EUROPEAN PARLIAMENT AND OF THE COUNCIL amending Directive 2012/27/EU on energy efficiency COM/2016/0761 final - 2016/0376 (COD); 2016.
[3] Frijns J, Hofman J, Nederlof M. The potential of (waste) water as energy carrier. Energ Conver Manage 2013;65:357–63.
[4] Lapertot A, Segond G, Fasquelle T, Kadoch B, Le Metayer O. Multi-criteria optimization of an experimental system for the production of domestic hot water. Energ Conver Manage 2022;267:115875.
[5] Marszal-Pomianowska A, Zhang C, Pomianowski M, Heiselberg P, Gram-Hanssen K, Hansen AR. Simple methodology to estimate the mean hourly and the daily profiles of domestic hot water demand from hourly total heating readings. Energ Buildings 2019;184:53–64.
[6] Pomianowski MZ, Johra HH, Marszal-Pomianowska A, Zhang C. Sustainable and energy-efficient domestic hot water systems: A review. Renew Sustain Energy Rev 2020;128:109900.
[7] Marini D, Buswell R, Hopfe C. «Estimating waste heat from domestic hot water systems in UK dwellings,» in *Int.* Hyderabad, India: Build. Perform. Simul. Assoc; 2015.
[8] Tiefenbeck V, Goette L, Degen K, Tasic V, Fleisch E, Lalive R, et al. Overcoming salience bias: How real-time feedback fosters resource conservation. Manag Sci 2018;64(3):983–1476.
[9] Huber F, Neugebauer G, Ertl T, Kretschmer F. Suitability Pre-Assessment of in-Sewer Heat Recovery Sites Combining Energy and Wastewater Perspectives. Energies 2020;13(24):6680.
[10] Nagpal H, Spriet J, Murali M, McNabola A. Heat recovery from wastewater - a review of available resource. Water 2021;13(9):1274.
[11] Piotrowska B, Słys D. «Variant analysis of financial and energy efficiency of the heat recovery system and domestic hot water preparation for a single-family building: The case of Poland,» *Journal of Building.* Engineering 2023;65:105769.
[12] Bøhm B. Production and distribution of domestic hot water in selected Danish apartment buildings and institutions. Analysis of consumption, energy efficiency and the significance for energy design requirements of buildings. Energ Conver Manage 2013;67:152–9.
[13] Valdiserri P. Evaluation and control of thermal losses and solar fraction in a hot water solar system. International Journal of Low-Carbon Technologies 2018;13(3):260–5.
[14] Cholewa T, Siuta-Olcha A, Anasiewicz R. On the possibilities to increase energy efficiency of domestic hot water preparation systems in existing buildings-long term field research. J Clean Prod 2019;217:194–203.
[15] Binks AN, Kenway SJ, Lant PA. The effect of water demand management in showers on houshold energy use. J Clean Prod 2017;157:177–89.
[16] Lee JY, Yim T. Energy and flow demand analysis of domestic hot water in an apartment complex using smart meter. Energy 2021;229:120678.
[17] Niemela T, Manner M, Laitinen A, Sivula TM, Jokisalo J, Kosonen R. Computational and experimental performance analysis of a novel method for heating of domestic hot water with a ground source heat pump system. Energ Buildings 2018;161:22–40.
[18] Liu J, Zhou L, Lyu N, Lin Z, Zhang S, Zhang X. Analysis of a modified transcritical CO2 two-stage ejector-compression cycle for domestic hot water production. Energ Conver Manage 2022;269:116094.
[19] Liu H, Katsura T, Nagano K. «An inverter-driven heat pump with a multi-tubular tube-in-tube heat exchanger for domestic hot water supply,» *Journal of Building.* Engineering 2022;54:104694.
[20] Famiglietti J, Toppi T, Bonalumi D, Motta M. Heat pumps for space heating and domestic hot water production in residential buildings, an environmental comparison in a present and future scenario. Energ Conver Manage 2023;276:116527.
[21] Yang X, Li H, Svendsen S. Energy, economy and exergy evaluations of the solutions for supplying domestic hot water from low-temperature district heating in Denmark. Energy Conversion and Managements 2016;122:142–52.
[22] Huang T, Yang X, Svendsen S. Multi-mode control method for the existing domestic hot water storage tanks with district heating supply. Energy 2020;vol. 191:116517.
[23] Brottier L, Bennacer R. Thermal performance analysis of 28 PVT solar domestic hot water installations in Western Europe. Renew Energy 2020;160:196–210.
[24] Kalkan C, Duquette J, Ezan MA. Development of a novel computational fluid dynamics-based model for a solar photovoltaic/thermal collector-assisted domestic hot water system with sensible heat storage. Appl Therm Eng 2023;228:120424.
[25] Nair AM, Wilson C, Huang MJ, Griffiths P, Hewitt N. Phase change materials in building integrated space heating and domestic hot water applications: A review. J Storage Mater 2022;54:105227.
[26] Navarroa L, Barrenechea C, Castella A, Redpath DAG, Griffiths PW, Cabeza LF. High density polyethylene spheres with PCM for domestic hot water applications: Water tank and laboratory scale study. J Storage Mater 2017;13:262–7.
[27] Khoury S, Maatouk C, El Khoury K, Khatounian F. Optimization methodology of thermal energy storage systems for domestic water heating applications with different configurations. J Storage Mater 2022;50:104530.
[28] Yang M, Moghimi MA, Loillier R, Markides CN, Kadivar M. Design of a latent heat thermal energy storage system under simultaneous charging and discharging for solar domestic hot water applications. Appl Energy 2023;336:120848.
[29] Hadengue B, Morgenroth E, Larsen TA. Screening innovative technologies for energy-efficient domestic hot water systems. J Environ Manage 2022;320:115713.
[30] *e*-SAFE, (Energy and Seismic AFfordable rEnovation solutions) project. https://esafe-buildings.eu/en/ .
[31] Kottek M, Grieser J, Beck C, Rudolf B, Rubel F. World Map of the Köppen-Geiger climate classification updated. Meteorol Z 2006;15(3):259–63.
[32] European Committee for Standardization 2012.

[33] European Committee for Standardization 2000.
[34] Fuentes E, Arce L, Salom J. A review of domestic hot water consumption profiles for application in systems and buildings energy performance analysis. Renew Sustain Energy Rev 2018;81:1530–47.
[35] Ivanko D, Walnum HT, Nord N. Development and analysis of hourly DHW heat use profiles in nursing homes in Norway. Energ Buildings 2020;222:110070.
[36] Knight I, Kreutzer N, Manning M, Swinton M. «European and Canadian non-HVAC electric demand and DHW load profiles for use in simulating the performance of residential cogeneration systems,» Energy conservation in buildings and community systems. IEA Annex 2007;42(6):84.
[37] De Simone M, Callea L, Fajilla G. Surveys and inferential statistics to analyze contextual and personal factors influencing domestic hot water systems and usage profiles in residential buildings of Southern Italy. Energ Buildings 2022;255:111660.
[38] UNI/TS 11300-4: Energy performance of buildings: Part. 4 Renewable energy and other generation systems for space heating and domestic hot water production, UNI, 2016.
[39] DPR412/93, «DPR 26 agosto 1993, n. 412. Regolamento recante norme per la progettazione, l'installazione, l'esercizio e la manutenzione degli impianti termici degli edifici, in Attuazione dell'art. 4, comma 4, della L. 9 gennaio 1991, n. 10;,» President of the Italian Republic:, Roma, Italy (In Italian), 1993.
[40] European Commission, «JRC Photovoltaic Geographical Information System (PVGIS),» https://re.jrc.ec.europa.eu/pvg_tools/en/.
[41] «Indicazioni metodologiche per l'applicazione dei fattori di conversione al metodo di calcolo di cui alla DGR 967/2015 e alla DGR 1275/2015,» Regione Emilia-Romagna (in Italian), 2015.
[42] Callefi, Idraulica - Publicazione periodica di informazione tecnico-professionale (in Italian), 53, 2017.
[43] Jahanbin A, Valdiserri P, Semprini G. Multi-objective study on an innovative system for domestic hot water production: A pilot building in Southern Europe. Energ Buildings 2023;293:113181.
[44] Perez-Fargallo A, Bienvenido-Huertas D, Contreras-Espinoza S, Marín-Restrepo L. «Domestic hot water consumption prediction models suited for dwellings in central-southern parts of Chile,» *Journal of Building.* Engineering 2022;49:104024.
[45] Stec A, Sabina Kordana S, Słys D. Analysing the financial efficiency of use of water and energy saving systems in single-family homes. J Clean Prod 2017;151:193–205.
[46] Liu W, Chen C, Wu H, Guo C, Chen Y, Liu W, et al. Environmental life cycle assessment and techno-economic analysis of domestic hot water systems in China. Energy Conversion and Managment 2019;199:111943.
[47] Statista, https://www.statista.com/statistics/1267548/italy-monthly-wholesale-electricity-price/ [Online].
[48] Water News Europe, https://www.waternewseurope.com/water-prices-compared-in-36-eu-cities/ [Online].
[49] UNI/TS 11300-1: Energy performance od buildings: Part.1 Evaluation of energy need for space heating and cooling, UNI; 2014.
[50] Evola G, Costanzo V, Urso A, Tardo C, Margani G. Energy performance of a prefabricated timber-based retrofit solution applied to a pilot building in Southern Europe. Build Environ 2022;222:109442.